ARTICLE

BIOTECHNOLOGY AND BIOENGINEERING

Novel Iron–Sulfur Containing NADPH-Reductase From *Nocardia farcinica* IFM10152 and Fusion Construction With CYP51 Lanosterol Demethylase

Kwon-Young Choi,[1] Eun-Ok Jung,[1] Da-Hye Jung,[1] Bishnu Prasad Pandey,[1] Nahum Lee,[1] Hyungdon Yun,[2] Hyung-yun Park,[3] Byung-Gee Kim[1]

[1]School of Chemical and Biological Engineering, Institute of Bioengineering, Seoul National University, Seoul, South Korea; telephone: +82-2-880-6774; fax: +82-2-874-1206; e-mail: byungkim@snu.ac.kr

[2]School of Biotechnology, Yeungnam University, Gyeongsan, Gyeongbuk, South Korea

[3]Korea Bio-Hub Center, Bio-MAX Institute, Seoul National University, Seoul, South Korea

Received 10 May 2011; revision received 4 October 2011; accepted 17 October 2011

Published online 28 October 2011 in Wiley Online Library (wileyonlinelibrary.com). DOI 10.1002/bit.24359

ABSTRACT: CYP51, a sterol 14α-demethylase, is one of the key enzymes involved in sterol biosynthesis and requires electrons transferred from its redox partners. A unique CYP51 from *Nocardia farcinica* IFM10152 forms a distinct cluster with iron–sulfur containing NADPH-P450 reductase (FprD) downstream of CYP51. Previously, sequence alignment of nine reductases from *N. farcinica* revealed that FprC, FprD, and FprH have an additional sequence at their N-termini that has very high identity with iron–sulfur clustered ferredoxin G (FdxG). To construct an artificial self-sufficient cytochrome P450 monooxygenase (CYP) with only FprD, CYP51, and iron–sulfur containing FprD were fused together with designed linker sequences. CYP51–FprD fusion enzymes showed distinct spectral properties of both flavoprotein and CYP. CYP51–FprD F1 and F2 in recombinant *Escherichia coli* BL21(DE3) catalyzed demethylation of lanosterol more efficiently, with k_{cat}/K_m values of 96.91 and 105.79 nmol/min/nmol, respectively, which are about 35-fold higher compared to those of CYP51 and FprD alone.

Biotechnol. Bioeng. 2012;109: 630–636.

KEYWORDS: CYP51; lanosterol demethylase; iron–sulfur containing flavoprotein; fusion protein

Introduction

Cytochrome P450 monooxygenases (CYPs) are a superfamily of heme-thiolate-containing enzymes, which catalyze a variety of chemical reactions in regio- and stereo-selective manners (Isin and Guengerich, 2007; Sono et al., 1996). More than 40 different types of reactions catalyzed by CYPs have been identified. Generally, these enzymes act as monooxygenases, introducing an oxygen molecule into a substrate molecule whereby one atom of molecular oxygen is incorporated into the product (Sono et al., 1996). Among the various families of CYPs in bacteria, CYP51 is a unique enzyme that catalyzes oxidative modification reaction of steroids, thus allowing sterol metabolism to synthesize an end-product, such as cholesterol, ergosterol, and phytosterol (Lepesheva et al., 2006; Rozman 2000). The preferred substrate of CYP51 in bacteria is lanosterol, and most bacterial CYP51 are known to catalyze oxidative removal of its 14α-methyl group via a three-step oxidation process (Aoyama 2005; Jackson et al., 2003; Lepesheva and Waterman 2004).

Despite the fascinating catalytic activities of CYP51 family enzymes, their major limitation is their requirement of an electron transfer system (Hannemann et al., 2007; Munro et al., 2007; O'Reilly et al., 2011), especially ferredoxin (Fdx) and NAD(P)H-dependent Fdx reductase are essential for class I type of bacterial CYPs. One exception, however, are self-sufficient CYPs containing NAD(P)H-Fdx reductase in a single peptide, which have been well documented elsewhere (Munro et al., 2002; Urlacher et al., 2004, 2008). Until now, four different fusion systems of CYPs have been reported. The most abundant type is bacterial [CYP]–[CPR] fusion system where heme domain is fused with diflavin (FMN/FAD)-containing reductase such as CYP102A1 (P450BM3, EC 1.14.14.1; O'Reilly et al., 2011). This type of CYPs is composed of a heme domain connected via a short protein linker to a diflavin reductase domain. The other fusion type is rather rare, bacterial [Fdx]–[CYP], bacterial [Fldx]–[CYP], and bacterial [PFOR]–[CYP] fusion system, wherein heme domains are fused with a domain of iron–sulfur containing Fdx, flavodoxin domain, and highly similar to phthalate family oxygenase reductase (PFOR),

Correspondence to: B.-G. Kim

Additional Supporting Information may be found in the online version of this article.

respectively. Especially in bacterial [Fdx]–[CYP] fusion system, electrons flow like in the class I bacterial system from NAD(P)H via a flavin and iron–sulfur redox center to heme (Hannemann et al., 2007). As fusion arrangement enhances electron transfer efficiency, and thereby catalytic efficiency in terms of kinetic parameters (k_{cat}, K_m), many groups have reported new self-sufficient CYPs or genetically modified artificial self-sufficient CYPs (Narhi and Fulco, 1986).

Here, we report a CYP51 identified in *N. farcinica* (Ishikawa et al., 2004) clustered with NADPH-dependent (iron–sulfur containing) Fdx reductase. This novel reductase was found to be very rare in prokaryote CYP systems and consist of two distinct domains, iron–sulfur cluster (4Fe–4S)-binding domain and FAD-binding domain, suggesting that it was naturally fused or fused during its evolutionary history with Fdx and iron–sulfur cluster Fdx reductase. Although many chimera constructions have been reported using diflavin-containing NADPH-reductases (Dodhia et al., 2006; Mattheos and Koffas, 2007; Seliskar et al., 2008), this is the first report on the fusion of a class I type of bacterial CYP51 with an iron–sulfur-containing NAD(P)H-reductase of which structure organization is similar to PFOR consisted of both flavin and iron–sulfur clusters.

Materials and Methods

Chemicals

Lanosterol was purchased from Sigma–Aldrich Chemical Co. (St. Louis, MO). *N,O-bis*(trimethylsily)trifluoroacetamide for derivatization and GC/MS analysis was purchased from Fluka (Buchs, Switzerland). All other chemicals were of the highest grade available.

Plasmids Construction and Generation of Fusion Protein

Chromosomal DNA from *N. farcinica* IFM10152 was prepared using a G-spin^{TM} genomic DNA extraction kit (iNtRon Biotechnology Inc., Sungnam, South Korea). CYP51 and ferredoxin reductase gene (FprD) were amplified from the bacterial genome by PCR using sets of specific primers. The PCR reaction conditions were as follows: 30 cycles of denaturation for 30 s at 94°C, annealing for 1.5 min from 65 to 72°C, and extension for 30 s at 72°C. The PCR products were cloned into pET-24ma(+) expression vector, respectively (Novagen, Madizson, WI).

The strategy for constructing the expression vector for the fusion proteins containing CYP51 and FprD involved insertion of a set of linkers. The first fusion protein CYP51–FprD F1 consisted of CYP51, a linker region containing the amino acid sequence STEQSAKEAPAETLGAFR and FprD. The expression vector (pET24ma(+)) for F1 was constructed by inserting CYP51 DNA, in which the C-terminus was additionally modified by tagging tcg/acc/gaa/cag/tcg/gcg/aaa sequences using a set of primers. Finally, the FprD-encoding DNA, in which the N-terminus was additionally modified by tagging gaa/gcg/ccg/gcg/gaa/acc/ctg/ggc/gcg/ttt/cgc using a set of primers, was cloned again into pET24ma(+)::CYP51-STEQSA plasmid. Further, the second fusion protein CYP51–FprC F2 consisted of CYP51, a linker region containing the amino acid sequence AAVDAKASAGEAPAETLGAFR and FprD. The expression vector (pET24ma(+)) for F2 was constructed by inserting CYP51 DNA, in which the C-terminus was additionally modified by tagging gcg/gcg/gtg/gat/gcg/aaa/gcg/tcg/gcg/ggc sequence using a set of primers. Finally, the FprD-encoding DNA, in which the N-terminus was additionally modified by tagging gaa/gcg/ccg/gcg/gaa/acc/ctg/ggc/gcg/ttt/cgc using a set of primers, was cloned again into pET24ma(+)::CYP51-AAVDAKASAG plasmid.

Expression and Purification of CYP5, FprD, and CYP51–FprD Fusion Enzymes (F1 and F2)

Each plasmid was transformed into *Escherichia coli* BL21 (*DE3*). The transformants were grown in terrific broth (TB) medium containing 50 μg/mL of kanamycin at 37°C until an $OD_{600\,nm}$ of 0.6. Isopropyl-thio-β-D-galactopyranoside (IPTG) along with 0.5 mM of δ-aminolevulinic acid as a heme precursor was then added up to a final concentration of 0.01 mM, after which cells were grown at 30°C for 12 h. Cells were then harvested by centrifugation and washed twice with ice-cold PBS buffer. Cells resuspended in potassium phosphate buffer (pH 7.2) were used for the isolation of proteins.

Centrifuged cells were resuspended in 5 mL of sonication buffer composed of 10 mM Tris–HCl (pH 7.0), 2 mM EDTA, 1 mM PMSF, and 0.01% (v/v) 2-mercaptoethanol, and then disrupted by sonication. The disrupted soluble fraction was collected by centrifugation and then purified using a Ni-NTA His-tag purification kit. Purified proteins were subjected to in vitro enzyme reactions and SDS–PAGE, and spectrophotometric analysis was used to measure CO-binding activity.

Chromatographic Determination of Flavin and Reductase Domain Activity

To release flavin from iron–sulfur containing Fdx reductase, the reductase protein was denatured at 60°C for 60 min and isolated as described by Liu and Urlacher (2006)). Using flavin adenine dinucleotide (FAD) as a control, flavin was separated by TLC analysis on a silica gel plate. The TLC plate was visualized by exposure to UV light (254 nm).

To identify the preferred cofactor, the NADH and NADPH consumption rates were determined using 1 μL of 2.5 μM CYP mixed with 89 μL of 0.1 M potassium phosphate buffer (pH 7.0) containing 1.0 μg of cytochrome *c*. After addition of each cofactor, consumption was monitored at 340 nm by UV/vis spectrometry (Thermo

Labsystems) at room temperature every 20 s. The NADPH concentration was calculated using an extinction coefficient of 6,200 M/cm.

UV/Visible Characteristic Features of CYP51 and Fusion Proteins (F1 and F2)

UV absorption spectra of CO-bound recombinant CYP proteins after sodiumdithionite reduction were measured by UV spectrometry (Spectronic, Genesys) by scanning the wavelength from 350 to 600 nm. The concentration of each protein was measured based on the CO difference spectra using an extinction coefficient of 91 mM/cm at 450 nm (Omura and Sato, 1964).

HPLC and GC/MS Analysis of Products

Lanosterol reaction metabolites were separated by HPLC equipped with a C18 reverse phase column (Waters, 4.6 mm × 150 mm, Symmetry® C18 5.0) and eluted at 0.8 mL/min with ACN/Water solution (20:80 v/v) containing 0.1% trifluoroacetic acid. The absorbance of the eluent was monitored at 254 nm.

For structural analysis, the reaction products were separated and their corresponding mass spectra analyzed by GC/MS. To protect hydroxyl groups, lanosterol and its reaction products were derivatized using BSTFA (*N*,*O*-*bis*(trimethylsilyl)trifluoroacetamide) by heating at 60°C for 60 min. GC/MS was performed using a Thermo Ultra Trace GC system (Gas chromatograph model ITQ110 GC-ion Trap; Thermo Science) connected to an ion trap mass detector. The BSTFA derivatives were separated in a nonpolar capillary column (5% phenyl methyl siloxane capillary 30 m × 250 nm i.d., 0.24 μm film thickness) containing a linear temperature gradient (at 60°C, hold for 1 min; 20°C/min to 250°C, hold for 10 min; 1°C/min to 275°C, hold for 3 min; Trosken et al., 2004). The injector port temperature was 260°C. Mass spectra were obtained by electron impact ionization at 70 eV, and scan spectra were obtained within the range of 100–600 *m*/*z*. Selected ion mode (SIM) was used for the detection and fragmentation analysis of lanosterol as well as its reaction metabolites.

Determination of the Enzyme Activity of CYP51 Fusion Protein (F1 and F2)

The activity of reconstituted CYP51 and CYP51 fusion proteins were measured by monitoring the decrease in UV absorption at 340 nm using an UV/vis spectrometer (Thermo Labsystems). A solution containing 160 μL of potassium phosphate buffer (pH 7.0), 10 μL of substrates in DMSO (10–200 μM), and 1.5 μM enzyme solution in a 96-well microplate was incubated for 5 min. The reaction was initiated by the addition of 10 μL of 10 mM NADPH. To determine kinetic parameters, all data were fitted to the Michaelis–Menten equation by linear regression. For the reference sample, NADPH consumption rates were measured without substrate.

Determination of K_d Value of CYP51 Fusion Protein With Lanosterol

Spectroscopic substrate binding spectra were measured as previously described by Munro et al. Purified proteins were diluted to 1.0 μM with 100 mM potassium phosphate buffer (pH 7.2), and binding spectra were recorded after each substrate was added to the enzyme solution. The final substrate concentrations were between 2.5 and 100 μM. To determine K_d value, the reciprocal differences in absorption intensity between 350 and 415 nm were plotted against reciprocal substrate concentrations. To calculate the K_d value of the enzyme–substrate complex, the experimental data were fitted to a hyperbolic curve ($y = ax/(b + x)$) using a nonlinear regression procedure based on the Durbin–Watson algorithm in the Sigma Plot software.

Homology Modeling of FprD for Identification of Iron–Sulfur and Flavin Structures

Homology modeling of FprD was performed using 1LQT, 1LQU, 2C7G, and 1E1M from the PDB database as templates. The predicted 3D structure of FprD was constructed based on a comparative homology modeling method using the Genefold and Composer programs from the SYBYL software package (Tripos Associates, St. Louis, MO). The initial state model was energy-minimized by the conjugate gradient method at an energy gradient norm of 0.01 kcal/mol. Docking simulations of cofactors were performed using the FlexX program. All ligand structures were minimized using a Tripos force field until the RMS gradient decreased below 0.05.

Result and Discussion

Clustering and Sequence Analysis of CYP51 and Iron–Sulfur Containing NAD(P)H-Reductase

The structural organization of CYP51 in the *N. farcinica* genome revealed that the NAD(P)H-reductase gene-encoding FprD was localized down-stream of CYP51, forming the class I type CYP51 cluster according to CYP classification based on electron transfer systems. This suggests that the redox partner of CYP51 is likely to be FprD for the monooxygenase enzymatic reaction. We next investigated where the remaining Fdx redox partner, among the 6 Fdxs in the cell, is located. Interestingly, the domain structure of FprC, FprD, and FprH was somewhat different from the other Fdx NAD(P)H-reductases in the sense that 3 Fprs contained longer N-terminal sequences (Fig. 1). The additional sequences were highly conserved, approximately 85 amino acids, and motif searches revealed that the motif

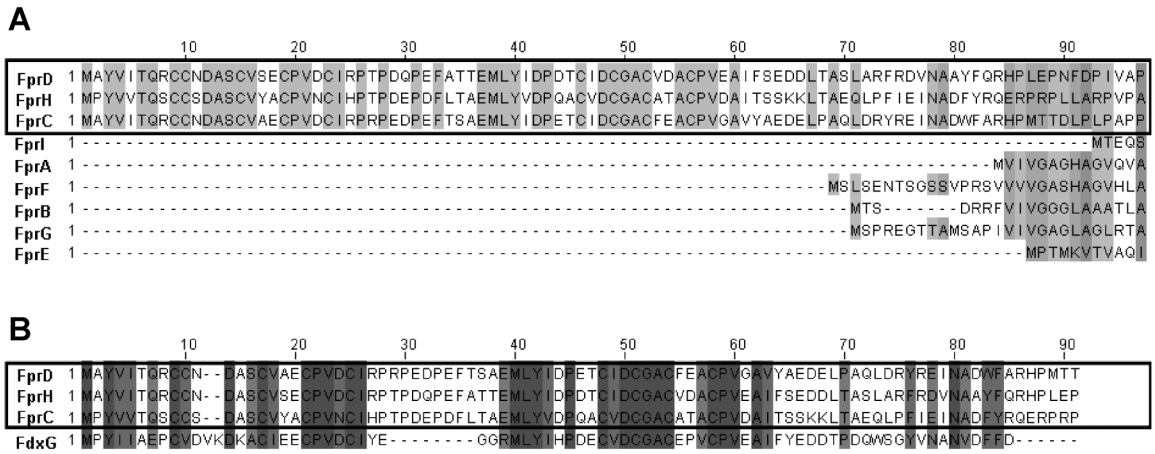

Figure 1. Sequence alignment of ferredoxin reductases from *Nocardia farcinica* IFM10152 and identification of additional sequences in the iron–sulfur domain by alignment with ferredoxins. **A**: Among the nine Fprs of *N. farcinica*, 3 Fprs (FprC, FprD, and FprH) contained an additional 85 amino acids at the N-terminus. Domain search revealed that they contained iron–sulfur (4Fe–4S) domains, which are generally found in ferredoxins. **B**: The partial sequences of the FprC, FprD, and FprH iron–sulfur domains were aligned with ferredoxins from *N. farcinica*, and FdxG showed the highest identity with partial sequences and they were highly conserved, approximately 85 amino acids, and motif searches revealed that the motif was similar to iron–sulfur (4Fe–4S)-binding domains with electron carrier activity similar to Fdxs.

was similar to iron–sulfur (4Fe–4S)-binding domains with electron carrier activity similar to Fdxs. The structure of these proteins consisted of two duplicated domains containing 26 amino acid residues with minor changes, and each domain contained four cysteine residues bound to a 4Fe–4S center (Yoshida et al., 1997). These members of the iron–sulfur cluster contained a similar conserved sequence of "C-x-{P}-C-x(2)-C-{CP}-x(2)-C-[PEG]," which is often found in various bacterial Fdxs, dehydrogenases, and reductases. Thus, the N-terminus of FprD appeared to be a fused moiety of Fdx from *N. farcinica*. Alignment further revealed that the extra N-terminal sequences in FprC/FprD/FprH had very high homology with FdxG, suggesting a possible evolutionary history of FprC/FprD/FprH with FdxG involving insertion, fusion, or duplication. All together, the sequence analysis results suggest that FprD does not belong to usual electron transfer partner for class I type of CYP, but instead to [Fdx]–[CPR] fusion type of reductases, which consist of a heme, FeS, and flavin (De Mot and Parret, 2002). This unusual gene organization and structure of iron–sulfur flavoprotein (FprD) and CYP51 motivated us to combine the two proteins together to generate an artificial fusion type of self-sufficient CYP51 and observe any improvement in catalytic activity (Nodate et al., 2006).

Functional Expression and Spectral Characterization of Fusion Protein (F1 and F2) With Flexible Linker

We fused CYP51 and FprD together by using two previously reported linkers, STEQSAKEAPAETLGAFR (F1 linker) from P450 BM3 and AAVDAKASAGEAPAETLGAFR (F2 linker) from P450foxy. Both P450 BM3 from *B. megaterium* and P450foxy from *Fusarium oxysporum* are fusion flavocytochromes belonging to class III. These linker peptides are known to form monomeric α-helices with approximately 80% helicity stabilized by Glu-Lys salt bridges, which is flexible enough to locate two separate domains and allow for efficient electron transfer. The two fused, artificial self-sufficient CYPs, termed F1 and F2, were constructed by gene manipulation.

Figure 2A shows the expression of the newly constructed fusion protein. All of the proteins, CYP51, FprD, and CYP51–FprD (F1 and F2), were expressed well as a soluble fraction, and His-tag purified proteins were prepared for in vitro reactions as a reconstituted system. The purified preparations of fusion proteins displayed a single protein band corresponding to a theoretical molecular weight of about 110 kDa, and the typical protein concentrations of the purified F1 and F2 proteins were 4.5 and 4.2 mg/mL, respectively.

To examine the functional folding of F1 and F2, the purified proteins in their ferric state (reduced form) were measured by UV/vis spectroscopy. In general, a cysteine–thiolate ligand coordinated to the heme iron atom of CYP regulates any spectroscopic and catalytic properties. Figure 2B shows the absorption spectra of F1 and F2. Asorption spectroscopy of purified CYP51 in its oxidized form (dashed line), reduced form (dash-dotted line), and substrate-binding form (solid line) revealed that CYP51 had general features typical of bacterial CYPs. In addition, the absorption spectra of the reduced-CO oxidized forms of F1 are indicated in the inset figure. The CO-difference spectra resulting from the insertion of CO gas into reduced F1 by sodium thionitrite show that the heme Soret absorption maxima was at 450 nm (Omura and Sato, 1964).

Flavin cofactor was identified by releasing flavin molecules after boiling purified F1 for 30 min. After

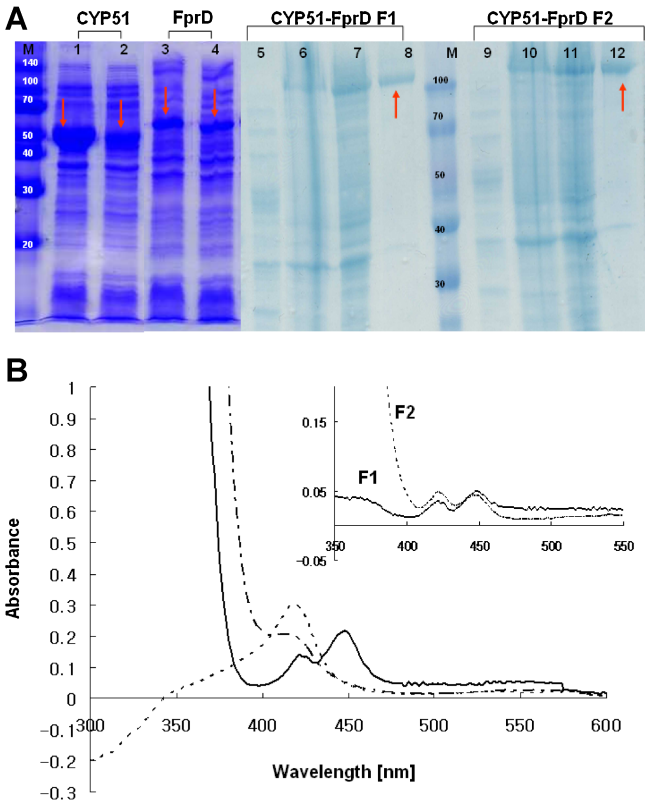

Figure 2. Expression and purification of CYP51, FprD, and CYP51–FprD reductase fusion protein in *E. coli* BL21 (DE3) cells, and evaluation of the catalytic activity of cytochrome P450. **A**: SDS–PAGE analysis of total cell protein content as well as purified protein containing 6-His tag; lane M: standard molecular weight markers; lane 1: total cell protein content of CYP51; lane 2: total soluble protein content of CYP51; lane 3: total cell protein content of FprD; lane 4: total soluble protein content of FprD; lane 5: total cell protein content of CYP51–FprD F1 before IPTG induction; lane 6: total cell protein content of CYP51–FprD F1; lane 7: total soluble protein content of CYP51–FprD F1; lane 8: purified protein content of CYP51–FprD F1; lane 9: total cell protein content of CYP51–FprD F2 before IPTG induction; lane 10: total cell protein content of CYP51–FprD F2; lane 11: total soluble protein content of CYP51–FprD F2; lane 12: purified protein content of CYP51–FprD F2. **B**: UV–visible absorbance spectra of purified CYP51 and CYP51–FprD reductase fusion protein revealed spectral features characteristic of CYPs; dashed line: oxidized form; dotted line: reduced form with dithionite; solid line: CO-difference spectra; inserted figure: CO-difference spectra of CYP51–FprD F1 and F2. [Color figure can be seen in the online version of this article, available at http://wileyonlinelibrary.com/bit]

centrifugation of the boiled solution, the supernatant containing flavin cofactor was analyzed by TLC. The supernatant sample displayed a single spot with an R_f value the same as that of the authentic standard FAD, suggesting the presence of flavin structures in the reductase domain of F1. To identify correct electron donors for the CYP enzyme reaction, NADPH and NADH were both used to measure the cytochrome *c* reductase activity of F1 and F2. CYP51–FprD fusion enzymes appeared to prefer NADPH (~600 μmol cyt *c*/min/μmol CYP) to NADH (~10 μmol cyt *c*/min/μmol CYP). The two CYP51–FprD fusion proteins showed turn-over numbers one order of magnitude lower than those of other self-sufficient bacterial CYPs such as BM3 (~6,000 μmol cyt *c*/min/μmol CYP; Munro et al., 2002).

Lanosterol 14α-Demethylation Catalyzed by CYP51 and CYP51–FprD Fusion Enzymes

The activities of both reconstituted CYP51 and CYP51–FprD fusion proteins were measured using lanosterol as a substrate. The reconstituted CYP51 and FprD enzyme reaction was carried out using CYP51 and FprD at a ratio of 1:1 based on protein concentration. GC-MS assay of lanosterol 14α-demethylase activity measured the 14α-demethylated product 4,4-dimethylcholesta-8,14,24-tiren-3-ol converted from lanosterol (Fig. 3). The kinetic parameters of the fusion F1 and F2 enzymes were comparable to those of the reconstituted CYP51 system with FprD (Table I), indicating that the fusion arrangement in a single polypeptide was efficient for intermolecular electron transfers rather than intramolecular electron transfers, thus good enough to for CYP activity and that the internal FdxG-like sequence was indeed functional for electron transfer as an Fe–S cluster. The K_d values of the reconstituted CYP51 and fusion F1 and F2 proteins were quite similar in the range of ~10 μM, whereas the catalytic activity (k_{cat}) of the fused enzymes was significantly different from that of CYP51 enzyme alone. The k_{cat} value of F1 and F2 was approximately 1,000 nmol/min/nmol of CYP, which is about 30-fold higher than that (40.17 nmol/min/nmol) of the reconstituted

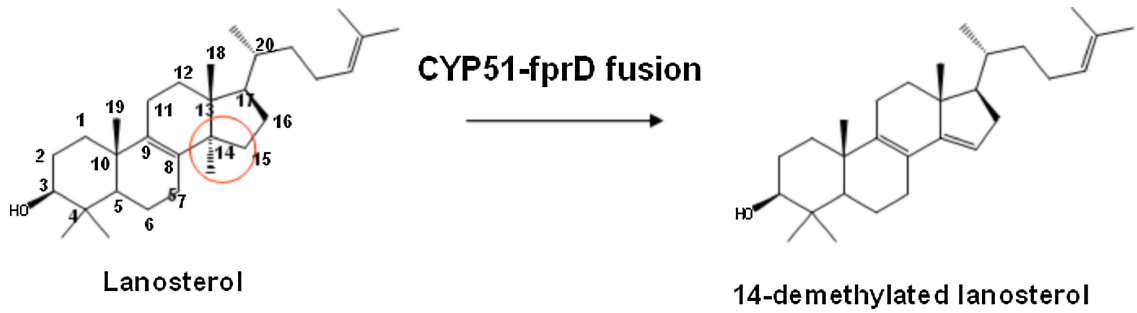

Figure 3. Oxidative metabolism of lanosterol by CYP51-reductase fusion enzyme. CYP51-reductase fusion enzyme catalyzes several steps of lanosterol oxidation and removes the methyl group at 14-position. [Color figure can be seen in the online version of this article, available at http://wileyonlinelibrary.com/bit]

Table I. Kinetic parameter comparison for lanosterol demethylation between CYP51 and CYP51–FprD fusion enzyme.

Kinetic parameters	CYP51	CYP51–FprD F1	CYP51–FprD F2
K_m (μM)	12.16	10.34	12.45
k_{cat} (min)	40.17	1002.05	1317.11
k_{cat}/K_m (μM/min)	3.03	96.91	105.79

Each substrate concentration was from 100 nM to 200 μM.

CYP51 system. These results indicate that the binding affinity between the heme domain of CYP51 and substrate lanosterol was not affected by fusion arrangement, whereas the fusion of CYP51 and FprD allowed effective intramolecular electron transfer from NADPH to the heme domain through reductase, confirming our expectations. Effective electron transfer between CYP and reductase existing in different molecules of a fusion monooxygenase could occur if the two molecules are dimeric partners, but this type of electron transfer cannot be discriminated from intramolecular transfer if the dissociation constant of the dimer is very small (Loida and Sligar, 1993). Such intermolecular electron transfer has been reported for naturally occurring bacterial fusion CYP enzymes such as CYP102A family members catalyzing fatty acid hydroxylation.

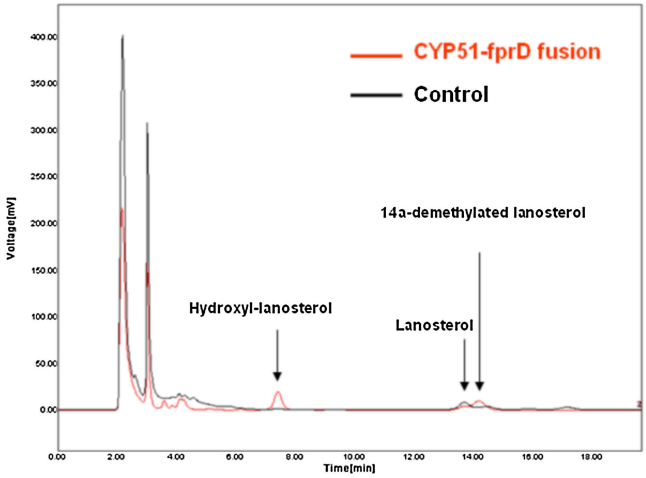

Figure 4. HPLC separation of lanosterol metabolites formed during incubation of 100 μM lanosterol with CYP51-rudctase fusion protein. Control: proteins were incubated without lanosterol, and lanosterol was detected at 13.9 min as a single fraction; Products: proteins were incubated with lanosterol; demethylated lanosterol was detected at 14.2 min and hydroxylated lanosterol was detected at 7.5 min. [Color figure can be seen in the online version of this article, available at http://wileyonlinelibrary.com/bit]

Quantitative and Structural Analysis of Reaction Products Using HPLC and GC/MS

Structural GC/MS analysis of demethylated lanosterol revealed that the methyl group of lanosterol at 14-position was removed, and an unsaturated double bond was formed during enzymatic reaction. Mass analysis of the trimethylsilylated (TMS)-derivatized product revealed peaks at 498 and 483 *m/z*, both of which matched well with the reference compound (Supplementary data). The *m/z* values of the product peak were equivalent to TMS-derivatized lanosterol, suggesting that the 483 *m/z* peak corresponded to $[M^+-15]$ ion (loss of CH_3 radical) resulting from the 498 *m/z* lanosterol peak. The demethylated product of lanosterol (483 *m/z* peak) was only observed as a major peak in the presence of CYP51 fusion protein after TMS derivatization (Supplementary data). As a control experiment for fragmentation pattern analysis, the 14-demethylated product of lanosterol bioconversion using a purified and reconstituted CYP51/FprD system was used.

HPLC separation of the lanosterol reaction products revealed an interesting result. One additional peak was detected in the presence of CYP51–FprD F1, which was not detected in the reconstituted CYP51 system (Fig. 4), suggesting that CYP51 contains both activities for lanosterol, hydroxylation, and demethylation. Further, GC/MS analysis revealed an unknown product with an ion mass of 587 and 572 *m/z*, indicating that it was the monohydroxylated product of CYP51–FprD F1 enzyme. However, the exact hydroxylated position was not clearly elucidated in spite of repeated mass fragment analysis using GC/MS^n.

Homology Modeling of Iron–Sulfur Containing NADPH-Reductase (FprD)

In this study, lanosterol was demethylated via several steps of oxidation by CYP51–FprD fusion enzymes, wherein an iron–sulfur FprD is responsible for transfer of a reducing equivalent from NADPH to CYP heme. Since this kind of electron transfer system is unusual in a CYP system, the combination of CYP51 and iron–sulfur FprD is somewhat unique in bacterial CYPs.

Computational simulation revealed that FprD had a modular structure in which FAD, NADPH, and [4Fe–4S]-binding sites were situated distinctively at the N-terminal, central, and C-terminal regions, respectively. As shown in Figure 5, the iron–sulfur cluster and flavin structures were incorporated together in the protein. Further, the iron–sulfur cluster consisted of two interleaved 4Fe- and 4S-tetrahedra forming a cubic structure in which the four irons occupied 4 out of 8 corners of a distorted cube. Each 4Fe–4S was attached to the polypeptide chain by four covalent Fe–S bonds with cysteine residues. Here, the flavin structure was located close to [4Fe–4S] within a calculated distance of 11.10 Å, which is very reasonable for the intermolecular transfer of electrons based on the distance (10–15 Å) between FAD and/or FMN found in most self-sufficient CYP structures (Noble et al., 1999). Although the conformational changes induced by interaction between FprD and CYP51 or substrate were not exactly predicted or calculated, sufficient electron transfer took place and enzymatic reactions occurred very quickly. For further investigation of this CYP-iron–sulfur FprD system, its

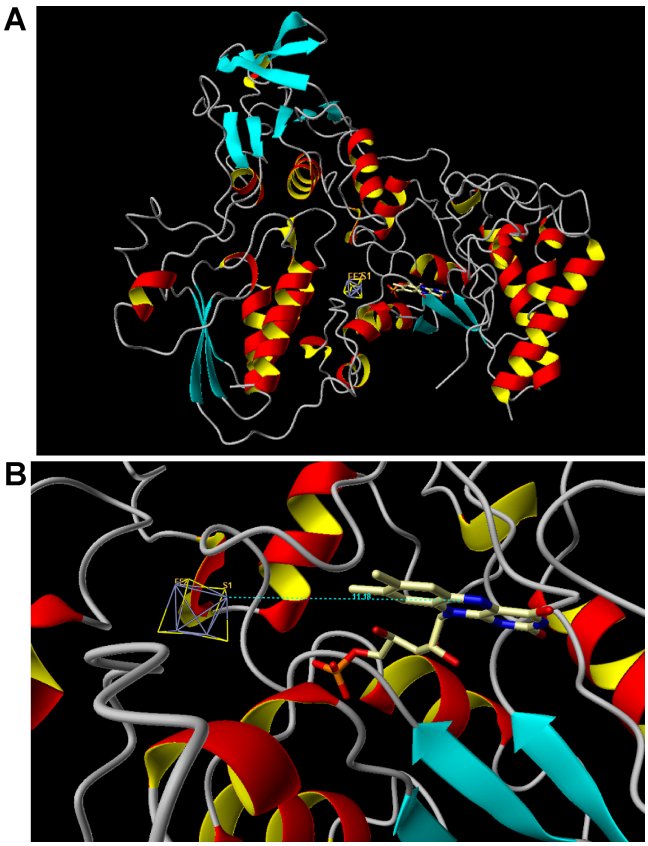

Figure 5. FprD structure containing (4Fe–4S) cluster sequence equivalent to Fdx was predicted by homology modeling. The binding motifs show two distinct domains separated into an iron–sulfur cluster and flavin structure. **A**: The full protein structure was predicted and cofactors, iron–sulfur cluster and flavin (FAD), were incorporated into the protein structure. **B**: Distance between (4Fe–4S) iron–sulfur cluster and FAD was 11.10 Å, as expected. [Color figure can be seen in the online version of this article, available at http://wileyonlinelibrary.com/bit]

electron transfer rate, and the coupling efficiency between the reconstituted and fused systems is being carried out.

References

Aoyama Y. 2005. Recent progress in the CYP51 research focusing on its unique evolutionary and functional characteristics as a diversozyme P450. Front Biosci 10:1546–1557.

De Mot R, Parret AH. 2002. A novel class of self-sufficient cytochrome P450 monooxygenases in prokaryotes. Trends Microbiol 10(11):502–508.

Dodhia VR, Fantuzzi A, Gilardi G. 2006. Engineering human cytochrome P450 enzymes into catalytically self-sufficient chimeras using molecular Lego. J Biol Inorg Chem 11(7):903–916.

Hannemann F, Bichet A, Ewen KM, Bernhardt R. 2007. Cytochrome P450 systems—Biological variations of electron transport chains. Biochim Biophys Acta 1770(3):330–344.

Ishikawa JYA, Mikami Y, Hoshino Y, Kurita H, Hotta K, Shiba T, Hattori M. 2004. The complete genomic sequence of *Nocardia farcinica* IFM 10152. Proc Natl Acad Sci USA 101(41):14925–14930.

Isin EM, Guengerich FP. 2007. Complex reactions catalyzed by cytochrome P450 enzymes. Biochim Biophys Acta 1770(3):314–329.

Jackson CJ, Lamb DC, Marczylo TH, Parker JE, Manning NL, Kelly DE, Kelly SL. 2003. Conservation and cloning of CYP51: A sterol 14 alpha-demethylase from *Mycobacterium smegmatis*. Biochem Biophys Res Commun 301(2):558–563.

Lepesheva GI, Waterman MR. 2004. CYP51—The omnipotent P450. Mol Cell Endocrinol 215(1–2):165–170.

Lepesheva GI, Hargrove TY, Ott RD, Nes WD, Waterman MR. 2006. Biodiversity of CYP51 in trypanosomes. Biochem Soc Trans 34(Pt 6):1161–1164.

Liu LSR, Urlacher VB. 2006. Cloning, expression, and characterization of a self-sufficient cytochrome P450 monooxygenase from *Rhodococcus ruber* DSM 44319. Appl Microbiol Biotechnol 72(5):876–882.

Loida PJ, Sligar SG. 1993. Molecular recognition in cytochrome P-450: Mechanism for the control of uncoupling reactions. Biochemistry 32(43):11530–11538.

Mattheos AG, Koffas EL. 2007. Engineering of artificial plant cytochrome P450 enzymes for synthesis of isoflavones by *Escherichia coli*. Appl Environ Microbiol 73(22):7246–7251.

Munro AW, Leys DG, McLean KJ, Marshall KR, Ost TW, Daff S, Miles CS, Chapman SK, Lysek DA, Moser CC, et al. 2002. P450 BM3: The very model of a modern flavocytochrome. Trends Biochem Sci 27(5):250–257.

Munro AW, Girvan HM, Mclean KJ. 2007. Cytochrome P450-redox partner fusion enzymes (review). Biocheim Biophys Acta 1770(3): 345–359.

Narhi LO, Fulco AJ. 1986. Characterization of a catalytically self-sufficient 119,000-dalton cytochrome P-450 monooxygease induced by barbiturates in *Bacillus megaterium*. J Biol Chem 261(16):7160–7169.

Noble MA, Miles CS, Chapman SK, Lysek DA, MacKay AC, Reid GA, Hanzlik RP, Munro AW. 1999. Roles of key active site residues in flavocytochrome P450 BM3. Biochem J 339(Pt 2):371–379.

Nodate M, Kubota M, Misawa N. 2006. Functional expression system for cytochrome P450 genes using the reductase domain of self-sufficient P450RhF from *Rhodococcus* sp. NCIMB 9784. Appl Microbiol Biotechnol 71(4):455–462.

Omura T, Sato R. 1964. The carbon monoxide-binding pigment of liber microsomes, I. Evidence for its hemoproteins nature. J Biol Chem 239:2370–2478.

O'Reilly E, Kohler V, Flitsch SL, Turner NJ. 2011. Cytochromes P450 as useful biocatalysts: Addressing the limitations. Chem Commun (Camb) 47(9):2490–2501.

Rozman D. 2000. Lanosterol 14alpha-demethylase (CYP51)—A cholesterol biosynthetic enzyme involved in production of meiosis activating sterols in oocytes and testis—A minireview. Pflugers Arch 439(3 Suppl):R56–R57.

Seliskar M, Kosir R, Rozman D. 2008. Expression of microsomal lanosterol 14alpha-demethylase (CYP51) in an engineered soluble monomeric form. Biochem Biophys Res Commun 371(4):855–859.

Sono M, Roach MP, Coulter ED, Dawson JH. 1996. Heme-containing oxygenases. Chem Rev 96(7):2841–2888.

Trosken ER, Straube E, Lutz WK, Volkel W, Patten C. 2004. Quantitation of lanosterol and its major metabolite FF-MAS in an inhibition assay of CYP51 by azoles with atmospheric pressure photoionization based LC-MS/MS. J Am Soc Mass Spectrom 15(8):1216–1221.

Urlacher VB, Budde M, Maurer SC, Schmid RD. 2004. Cloning, expression and characterisation of CYP102A2, a self-sufficient P450 monooxygenase from *Bacillus subtilis*. Appl Microbiol Biotechnol 66(2):180–186.

Urlacher VB, Dietrich M, Eiben S, Asta C, Do TA, Pleiss J. 2008. Cloning, expression and characterisation of CYP102A7, a self-sufficient P450 monooxygenase from *Bacillus licheniformis*. Appl Microbiol Biotechnol 79(6):931–940.

Yoshida Y, Noshiro M, Aoyama Y, Kawamoto T, Horiuchi T, Gotoh O. 1997. Structural and evolutionary studies on sterol 14-demethylase P450 (CYP51), the most conserved P450 monooxygenase: II. Evolutionary analysis of protein and gene structures. J Biochem 122(6):1122–1128.